ELSEVIER

Thermochimica Acta 364 (2000) 121–132

thermochimica acta

www.elsevier.com/locate/tca

Thermal analysis of carbon fiber polymer-matrix composites by electrical resistance measurement

D.D.L. Chung*

Composite Materials Research Laboratory, Department of Mechanical & Aerospace Engineering, State University of New York at Buffalo, Buffalo, NY 14260-4400, USA

Received 14 March 2000; received in revised form 14 July 2000; accepted 14 July 2000

Abstract

Thermal analysis conducted on carbon fiber polymer-matrix structural composites by DC electrical resistance measurement provided information on structural transitions, residual stress, composite interfaces, the composite fabrication process, and thermal damage. The composites involved continuous carbon fibers in single fiber and laminate forms, together with thermoplastic and thermoset matrices. The experimental methods and data interpretation are covered in this review.

Keywords: Thermal analysis; Polymer-matrix composite; Carbon fiber; Electrical resistance; Electrical resistivity

1. Introduction

Thermal analysis refers to the analysis of a material through measurement of a quantity as a function of temperature. The quantity may be heat (as in the case of calorimetry, usually differential scanning calorimetry, or DSC [1–10]), weight (as in the case of thermogravimetry, i.e., thermogravimetric analysis, or TGA [11,12]), dimension (as in the case of dilatometry, i.e., thermomechanical analysis, or TMA [3,8,10]), dynamic mechanical properties such as loss tangent and storage modulus (as in the case of dynamic mechanical analysis, or DMA, i.e., dynamic thermomechanical analysis, or DTMA [3–6,9,10,12–16]), etc. Thermal analysis can provide information on structural transitions, specific heat, coefficient of thermal expansion (CTE), process kinetics, thermal stability and composition.

A method of thermal analysis, which has received relatively little attention involves measurement of the electrical resistance as a function of temperature [17–22]. This method requires the material to be electrically conducting. Thus, a polymer which is insulating is not suitable for this method. However, polymers containing electrically conducting fillers are conducting and are thus suitable for this method. An example of such a material is a polymer reinforced with continuous carbon fibers, which are conducting and render the composite high strength and high modulus, as required for lightweight structures. This paper is a review that uses this widely used structural composite material to illustrate the application of thermal analysis in the form of the measurement of electrical resistance as a function of temperature.

The measurement of electrical resistance is fast, nondestructive and simple in terms of the equipment, which may be portable. It is thus amenable to process monitoring in real time, even in the field. It provides information on structural transitions, residual stress,

* Tel.:+1-716-645-2593; fax: +1-716-645-3875.
E-mail address: ddlchung@acsu.buffalo.edu (D.D.L. Chung).

0040-6031/00/$ – see front matter
PII: S0040-6031(00)00631-6

composite interfaces, the composite fabrication process, and thermal damage.

2. Structural transitions and thermal stress

The polymer matrix of a composite material can undergo structural transitions such as glass transition, melting, cold-crystallization and solid-state curing. Although the polymer matrix is insulating, the effect of a structural transition on the fiber morphology (e.g., the fiber waviness) results in an increase in the electrical resistivity of the composite in the fiber direction, thereby allowing the resistance change to indicate a structural transition of the matrix [17,18].

Due to the mismatch in the coefficient of thermal expansion (CTE) between polymer and fiber and the fact that the composite is fabricated at an elevated temperature, thermal stress is reduced upon heating the composite and is increased upon cooling. The thermal stress leads to an increase in the degree of fiber waviness or a decrease in the degree of fiber alignment, thereby increasing the resistance in the fiber direction of the composite. Thus, the electrical resistance provides an indication of the thermal stress.

The glass transition and melting behavior of a thermoplastic polymer depends on the degree of crystallinity, the crystalline perfection and other factors [23–28]. Knowledge of this behavior is valuable for the processing and use of the polymer. This behavior is most commonly studied by DSC [23–28], although the DSC technique is limited to small samples and the associated equipment is expensive and not portable. As the degree of crystallinity and the crystalline perfection of a polymer depend on the prior processing of the polymer and the effect of a process on the microstructure depends on the size and geometry of the polymer specimen, it is desirable to test the actual piece (instead of a small sample) for the glass transition and melting behavior. The measurement of electrical resistance provides a technique for this purpose.

DSC is a thermal analysis technique for recording the heat necessary to establish a zero temperature difference between a substance and a reference material, which are subjected to identical temperature programs in an environment heated or cooled at a controlled rate [29]. The recorded heat flow gives a measure of the amount of energy absorbed or evolved in a particular physical or chemical transformation. The concept behind the electrical resistance technique is totally different from that of DSC. This technique involves measuring the DC electrical resistance when the polymer has been reinforced with electrically conducting fibers such as continuous carbon fibers. The resistance is in the fiber direction. The polymer molecular movements that occur at the glass transition and melting disturb the carbon fibers, which are much more conducting than the polymer matrix, and thus affect the electrical resistance of the composite in the fiber direction, thereby allowing the resistance change to indicate the glass transition and melting behavior.

Exposure of polyamides to heat and oxygen may cause changes in the physical and chemical characteristics due to thermal oxidative degradation [30] and thus changes in the mechanical properties. Prolonged annealing at a high temperature results in undesirable changes in the degree of crystallization and in the end groups, and may cause inter- and intra-molecular transamidation reactions, chain scission and cross-linking [31–36]. The electrical resistance technique is capable of studying the effect of annealing (in air at various temperatures below the melting temperature for various lengths of time) on the glass transition and melting behavior.

2.1. DSC analysis of Nylon-6-matrix composite

Fig. 1(a) shows the DSC thermogram of the as-received carbon fiber Nylon-6-matrix composite. The glass transition was not observed by DSC. T_m (melting temperature, as indicated by the peak temperature) was 218.5°C. Fig. 1b–f shows the effect of annealing time and temperature on the melting peak. The DSC results are summarized in Table 1 [17]. Since T_m and ΔH of as-received and 100°C (5 h) annealed samples were almost the same (Fig. 1(a) and (b)), it was attributed to the little change of the crystal perfection or the degree of crystallinity during annealing at 100°C for 5 h. Fig. 1(c) shows the DSC thermogram of the sample annealed at 180°C for 5 h. It reveals two endothermic melting peaks with peak temperatures of 216 and 195°C. The lower temperature peak may be because of the structural reorganization during annealing in which the amorphous portion partly developed crystallinity [24,37,38]. As the annealing time increased to 15 h (Fig. 1(d)), the high-temperature

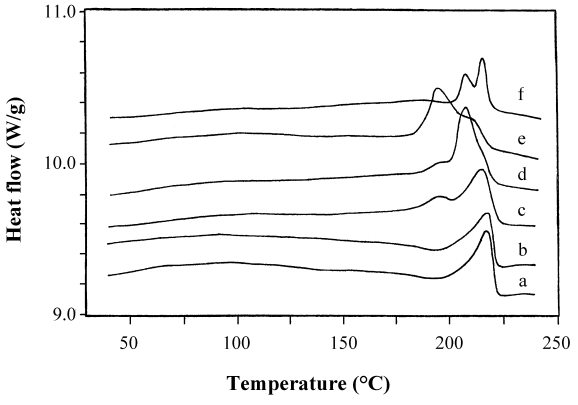

Fig. 1. DSC thermograms showing the melting endothermic peaks before and after annealing at the temperatures and for the times shown: (a) as-received; (b) 100°C, 5 h; (c) 180°C, 5 h; (d) 180°C, 15 h; (e) 180°C, 30 h; (f) 200°C, 5 h.

peak shifted to a lower temperature, but ΔH increased. As the annealing time increases to 30 h (Fig. 1(e)), the area of the low-temperature peak increased while that of the high-temperature peak decreased. These effects are probably due to the reorganization and thermal oxidative degradation of the Nylon-6 matrix, as explained below. When the annealing time increased from 5 (Fig. 1(c)) to 15 h (Fig. 1(d)), the degree of the crystallinity increased, so ΔH increased. However, at the same time, the extent of degradation increased due to thermal oxidation, which occurred during annealing at a high temperature (180°C), thus resulting in lower crystal perfection. Therefore, the high-temperature peak shifted to a lower temperature. When the annealing time was long enough (30 h, Fig. 1(e)), the crystalline portion from the reorganization process became dominant, as indicated by the increase of the area of the low-temperature peak. When the sample had been annealed at 200°C for 5 h (Fig. 1(f)), both T_m and ΔH decreased relative to the as-received sample. One possible explanation is that when the annealing temperature was very high, the extent of thermal degradation was extensive, resulting in less crystalline perfection as well as a lower degree of crystallinity.

2.2. Analysis of the DC electrical resistance for the Nylon-6-matrix composite

Fig. 2(a) [17] shows the fractional change in resistance for the as-received carbon fiber Nylon-6-matrix composite during heating, in which the temperature was raised from 25 to 350°C at a rate of 0.5°C/min. Two peaks were observed. The onset temperature of the first peak was 80°C and that of the second peak was 220°C. The first peak is attributed to matrix molecular movement above T_g; the second peak is attributed to matrix molecular movement above T_m. Because the molecular movement above T_g is less drastic than that above T_m, the first peak is much lower than the second one. As indicated before, the DSC thermogram of the as-received composite does not show a clear glass transition (Fig. 1(a)). Therefore, the resistance is more sensitive to the glass transition than DSC. The onset temperature (220°C) of the second peak (Fig. 2(a)) is higher than the onset temperature ($T_{onset} = 200.9$°C) of the DSC melting peak (Fig. 1(a)) and is close to the

Table 1
Calorimetry data for Nylon-6/CF composite before and after annealing

Annealing condition			T_{ml} (°C)[a]	T_{onset} (°C)[b]	T_m (°C)[c]	ΔH (J/g)[d]
Designation	Temperature (°C)	Time (h)				
a	[e]	[e]		200.9	218.5	26.7
b	100	5		205.5	218.2	26.6
c	180	5	194.8	201.3	215.5	34.8
d	180	15	196.3	201.4	208.9	39.1
e	180	30	196.3	200.0	209.0	38.6
f	200	5	208.3	212.9	216.4	16.5

[a] Peak temperature of the low-temperature melting peak.
[b] Onset temperature of the high-temperature melting peak.
[c] Peak temperature of the high-temperature melting peak.
[d] Heat of fusion.
[e] As-received.

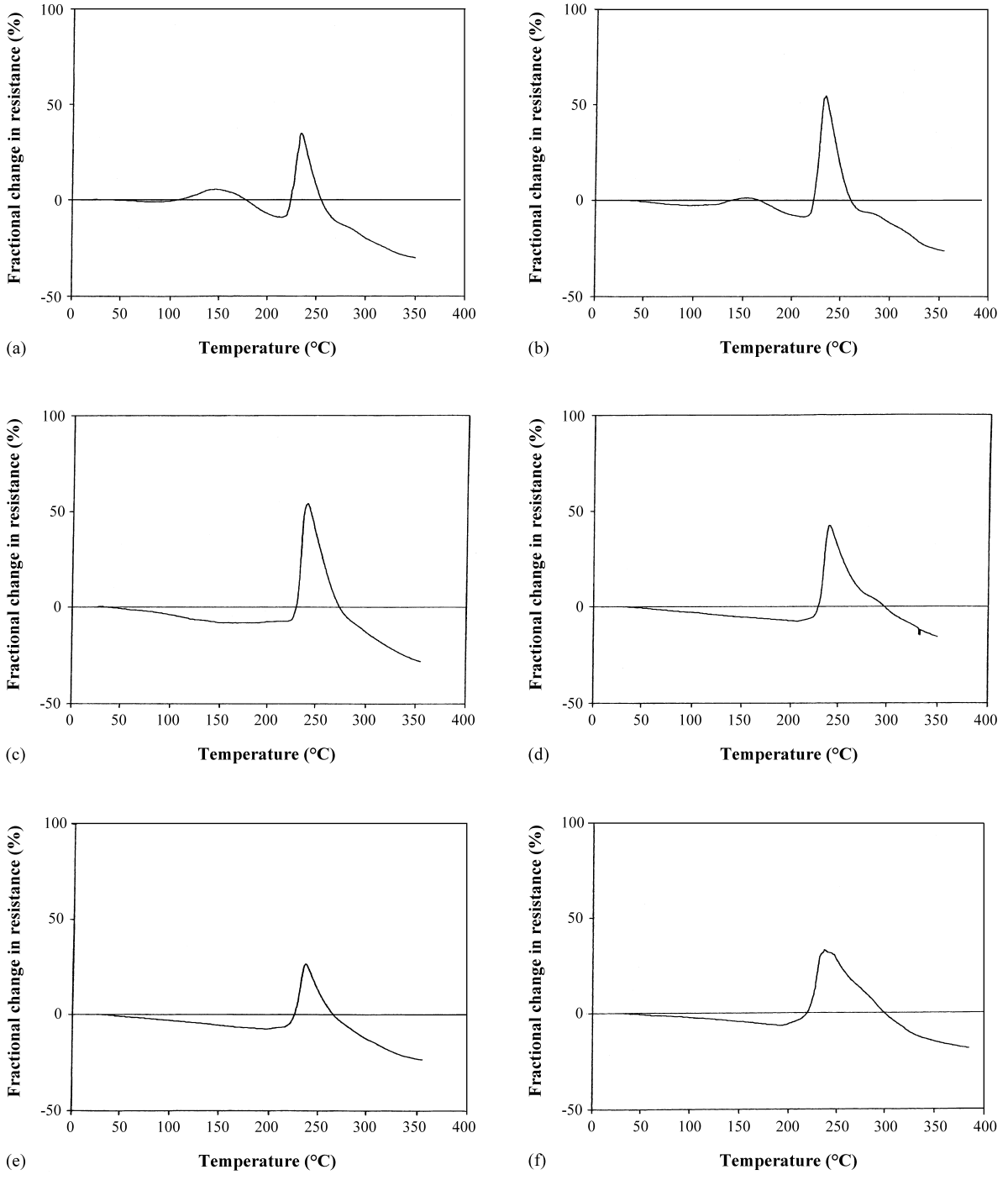

Fig. 2. Effect of annealing condition on the variation of the electrical resistance with temperature: (a) as-received; (b) 100°C, 5 h; (c) 180°C, 5 h; (d) 200°C, 5 h; (e) 180°C, 15 h; (f) 180°C, 30 h.

melting temperature ($T_m = 218.5°C$) indicated by DSC (Fig. 1(a)). The matrix molecular movement at T_{onset} is less intense than that at T_m, thereby giving no effect on the resistance curve at T_{onset}. Another reason may be a time lag between the matrix molecular movement and the resistance change.

Fig. 2(b)–(d) shows the effect of the annealing temperature. Comparison of Fig. 2(a) and (b) shows that annealing at 100°C for 5 h (Fig. 2(b)) had little effect on the glass transition and melting behavior of the Nylon-6 matrix; this is consistent with the DSC results (Fig. 1(a) and (b)). When the annealing temperature increased to 180°C (Fig. 2(c)), the peak due to molecular movement above T_g disappeared. This is attributed to the increase of the degree of crystallinity due to annealing. Because the crystalline portion has constraint on the molecular mobility, the higher the degree of crystallinity, the lesser is the possibility of molecular movement above T_g.

Not only does the degree of crystallinity but also the extent of thermal degradation affects the molecular mobility above T_g. Fig. 2(d) shows the fractional change in resistance of the sample annealed at 200°C for 5 h. No peak due to molecular movement above T_g was observed. The degree of crystallinity was less than that of the as-received sample, as shown by ΔH in Table 1. However, the higher extent of thermal degradation resulted in less molecular movement above T_g.

Fig. 2(c) and (e) shows the effect of annealing time from 5 to 15 h at 180°C. The height of the peak due to molecular movement above T_m decreased as the annealing time increased. A longer annealing time resulted in more thermal degradation of the matrix, which retarded the molecular movement above T_m. That this effect is due to a change of the extent of thermal degradation is also supported by the effect of annealing temperature, as shown in Fig. 2(c) and (d). A higher annealing temperature probably enhanced the extent of thermal degradation, thus resulting in a decrease of the height of the peak associated with molecular movement above T_m. Since the tail is more pronounced for samples with a larger extent of thermal degradation, as shown in Fig. 2(d) and (f), it may be attributed to the lower molecular mobility due to extensive thermal degradation.

2.3. Analysis of the DC electrical resistance for the polyphenylenesulfide-matrix composite

Fig. 3 [18] shows the fractional change in resistance of as-received carbon fiber polyphenylenesulfide (PPS)-matrix composite during the first two cycles of thermal cycling, in which the temperature was held at 235°C for 10 h in each cycle. The resistance increased abruptly during the first heating. During the subsequent period in which the temperature was held at 235°C, the resistance gradually decreased to

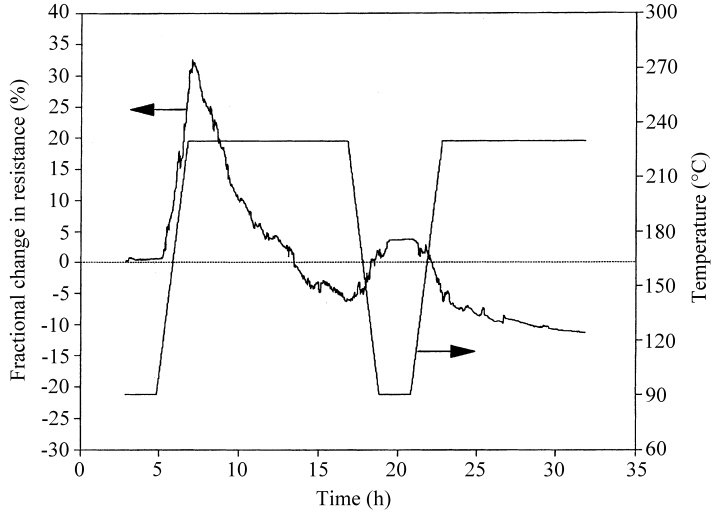

Fig. 3. Fractional change in electrical resistance during the first two cycles of thermal cycling for as-received composite.

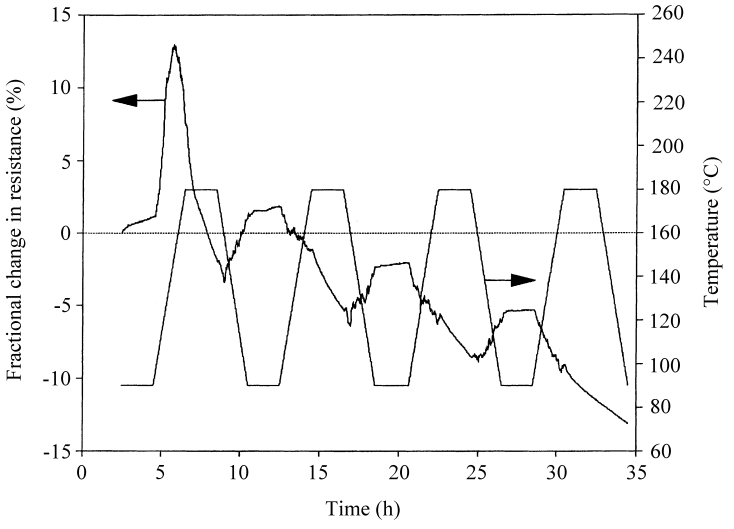

Fig. 4. Fractional change in electrical resistance during the first four cycles of thermal cycling for composite annealed at 180°C for 5 h.

levels below the initial resistance. During subsequent cooling, the resistance abruptly increased. During heating in the following cycle, the resistance decreased abruptly. The effect of cooling at the end of the first cycle on the resistance was reversed upon heating at the beginning of the second cycle. In the constant temperature (235°C) period of the second cycle, the resistance gradually decreased, as in the first cycle.

Fig. 4 [18] shows the fractional change in resistance of carbon fiber PPS-matrix composite that had been annealed at 180°C for 5 h during the first four cycles of thermal cycling, in which the temperature was held at 180°C for 2 h in each cycle. The resistance increased abruptly during the first heating, as in Fig. 3. During the subsequent period in which the temperature was held at 180°C, the resistance decreased to levels below the initial resistance. During subsequent cooling, the resistance increased. In every subsequent cycle, the resistance decreased during heating, decreased further during holding at 180°C to levels below the minimum resistance of the previous cycle, and increased during subsequent cooling. As cycling progressed, the resistance decrease in the 180°C constant temperature period became more and more gradual.

Fig. 5 [18] shows the fractional change in resistance of carbon fiber PPS-matrix composite that had been annealed at 180°C for 15 h during the first three cycles of thermal cycling, in which the temperature was held at 180°C for 10 h in each cycle. The resistance decreased abruptly during the first heating, in contrast to the abrupt increase in Figs. 3 and 4. Other than this, the pattern of resistance changes in Fig. 5 is the same as that in Figs. 3 and 4. However, the fractional changes in resistance are smaller in Fig. 5 than in Figs. 3 and 4.

The abrupt resistance increase during the first heating, observed only for the as-received composite and the composite annealed at 180°C for 5 h, is attributed to the poor bond between fiber and matrix and the resulting flow of the matrix during heating above T_g. The flow probably led to an increase in the degree of fiber waviness or a decrease in the degree of fiber alignment, thereby resulting in an increase in the resistance in the fiber direction of the composite. Annealing at 180°C for 15 h or more improved the fiber-matrix bond, thereby removing this effect. That this effect is due to matrix flow is also supported by the observation that flow (resistance increase) occurred at a constant temperature of 135°C, in addition to occurring during temperature increase.

The increase in resistance during cooling and decrease in resistance during subsequent heating (Figs. 3–5) are a reversible effect associated with the build-up of the thermal stress upon cooling and reduction of the thermal stress upon heating. The resistance decrease during first heating in Fig. 5 is also attributed to reduction in thermal stress.

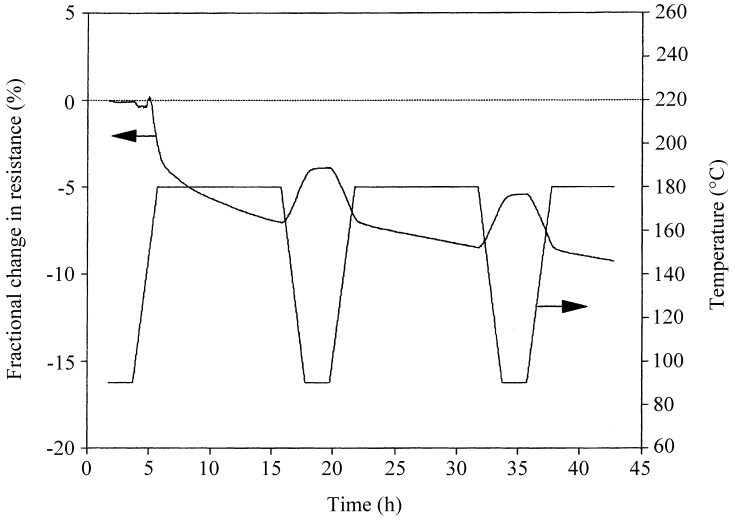

Fig. 5. Fractional change in electrical resistance during the first three cycles of thermal cycling for composite annealed at 180°C for 15 h.

The gradual decrease in resistance in the high temperature isothermal period of each cycle (Figs. 3–5) is attributed to crystallization of the matrix. Crystallization (known as transcrystallization) occurs on the fiber surface [39], thereby tending to decrease the fiber waviness. Hence, the resistance of the composite is decreased. The higher is the degree of crystallinity of the matrix, the lower is its resistance. Therefore, the minimum resistance of a cycle decreased cycle by cycle (Figs. 4 and 5). On the other hand, annealing at 180°C for 25 h (not shown) caused the crystallinity to essentially attain its maximum, so the above-mentioned effect due to crystallization essentially vanished. Annealing at 180°C for 15 h caused some crystallization (though not the maximum), so the above-mentioned effect due to crystallization is smaller in Fig. 5 than Figs. 3 and 4.

3. Interlaminar interface and thermal damage

The study of the interlaminar interface is commonly performed by measuring the interlaminar shear strength (ILSS) by techniques such as the short-beam method [40], the Iospiescu method [41] and other methods [42]. Although ILSS is a valuable quantity that describes the mechanical property of the joint between laminae, it gives little information on the interfacial structure, such as the extent of direct contact (with essentially no polymer matrix in between) between fibers of adjacent laminae and the residual interlaminar stress resulting from the anisotropy between adjacent laminae. The anisotropy is severe when the fibers in the adjacent laminae are in different directions, since the fibers and polymer matrix differ greatly in modulus and thermal expansion coefficient. Direct contact between fibers of adjacent laminae occurs due to the flow of the matrix during composite fabrication and the waviness of the fibers. Direct contact means that the thickness of the matrix between the adjacent fibers is so small (say, a few angstrom) that electrons can tunnel or hop from one fiber to the other. The presence of direct contact has been shown by the fact that the volume electrical resistivity of carbon fiber epoxy-matrix composites in the through-thickness direction is finite, even though the epoxy matrix is electrically insulating [43].

The contact electrical resistivity of the interlaminar interface can be used as a quantity to describe the structure of this interface [20,21]. Fig. 6 shows the variation of the contact resistivity ρ_c with temperature during reheating and subsequent cooling, both at 0.15°C/min, for samples cured at 0 and 0.33 MPa. The corresponding Arrhenius plots of log contact conductivity (inverse of contact resistivity) versus inverse absolute temperature during heating are shown in Fig. 7. From the slope (negative) of the Arrhenius plot, which is quite linear (not completely linear,

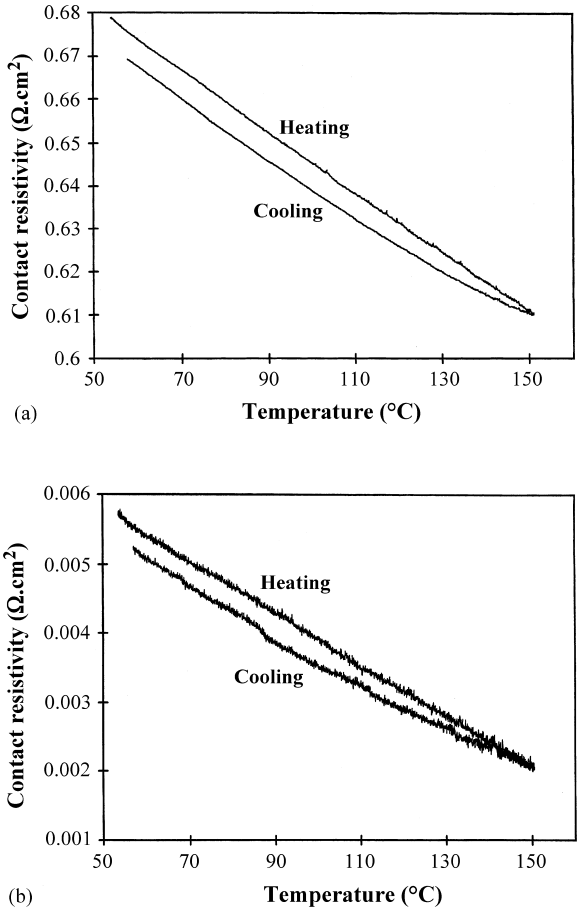

Fig. 6. Variation of contact electrical resistivity with temperature during heating and cooling at 0.15°C/min: (a) for sample made without any curing pressure and (b) for sample made with a curing pressure 0.33 MPa.

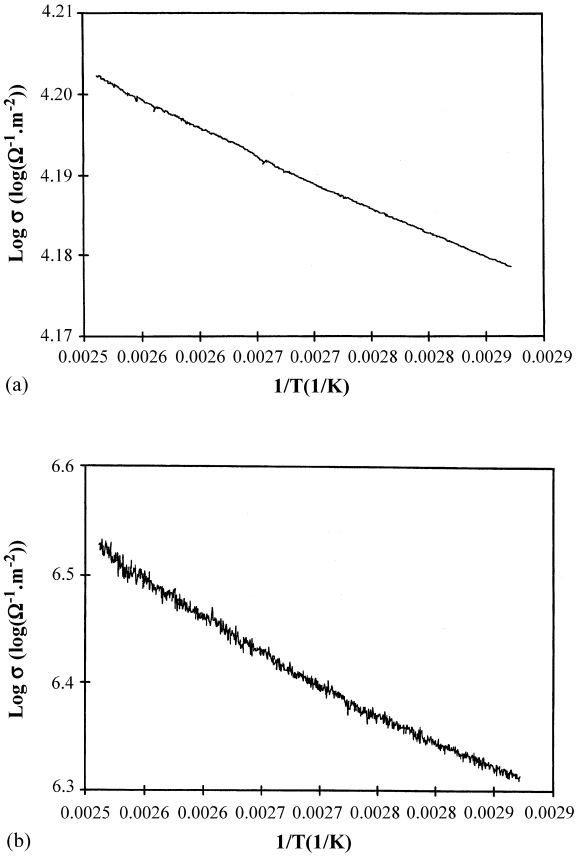

Fig. 7. Arrhenius plot of log contact conductivity vs. inverse absolute temperature during heating at 0.15°C/min: (a) for sample made without any curing pressure and (b) for sample made with curing pressure 0.33 MPa.

probably due to the effect of temperature on the microstructure), the activation energy can be calculated by using the equation

$$\text{slope} = -\frac{E}{2.3k}, \quad (1)$$

where k is the Boltzmann's constant, T the absolute temperature (in K), and E is the activation energy. The linearity of the Arrhenius plot means that the activation energy does not change throughout the temperature variation. This activation energy is the energy for electron jumping from one lamina to the other. Electronic excitation across this energy enables conduction in the through-thickness direction. This activation phenomenon is common in the electrical conduction of composite materials with an insulating matrix and an electrically conducting filler (whether particles or fibers). Based on volume resistivity measurement, an activation energy in the range from 0.060 to 0.069 eV has been previously reported for short carbon fiber polymer-matrix composites [44]. Direct measurement of the contact resistivity is impossible for the short fiber composites.

The activation energies, thicknesses and room temperature contact resistivities for samples made at different curing pressures and composite configurations are shown in Table 2. For the same composite configuration (crossply), the higher the curing pres-

Table 2
Activation energy for various composites[a]

Composite configuration	Curing pressure (MPa)	Composite thickness (mm)	Contact resistivity ρ_{co} (Ω cm^2)	Activation energy (eV)		
				Heating at 0.15°C/min	Heating at 1°C/min	Cooling at 0.15°C/min
Crossply	0	0.36	0.73	0.0131 (2×10^{-5})	0.0129 (3×10^{-5})	0.0125 (8×10^{-6})
	0.062	0.32	0.14	0.0131 (4×10^{-5})	0.0127 (7×10^{-5})	0.0127 (4×10^{-5})
	0.013	0.31	0.18	0.0168 (3×10^{-5})	0.0163 (4×10^{-5})	0.0161 (2×10^{-5})
	0.19	0.29	0.054	0.0222 (3×10^{-5})	0.0223 (3×10^{-5})	0.0221 (1×10^{-5})
	0.33	0.26	0.0040	0.118 (4×10^{-4})	0.129 (8×10^{-4})	0.117 (3×10^{-4})
Unidirectional	0.42	0.23	0.29	0.0106 (3×10^{-5})	0.0085 (4×10^{-5})	0.0081 (2×10^{-5})

[a] The standard deviations are shown in parentheses.

sure, the smaller is the composite thickness (because of more epoxy being squeezed out), the lower is the contact resisitivity, and the higher is the activation energy. A smaller composite thickness corresponds to a higher fiber volume fraction in the composite. During curing and subsequent cooling, the matrix shrinks while the carbon fibers essentially do not, so a longitudinal compressive stress will develop in the fibers. For carbon fibers, the modulus in the longitudinal direction is much higher than that in the transverse direction. Thus, the overall shrinkage in the longitudinal direction tends to be less than that in the transverse direction. Therefore, there will be a residual interlaminar stress in the two crossply layers in a given direction. This stress accentuates the barrier for the electrons to jump from one lamina to the other. The greater the residual interlaminar stress, the higher is the barrier, which is the activation energy. After curing and subsequent cooling, heating will decrease the thermal stress, due to the CTE mismatch between fibers and matrix. Both the thermal stress and the curing stress contribute to the residual interlaminar stress. Therefore, the higher the curing pressure, the larger is the fiber volume fraction, the greater is the residual interlaminar stress, and the higher the activation energy, as shown in Table 2. Most of the values of the activation energy shown in Table 2 are less than kT (where k is the Boltzmann's constant and T is the absolute temperature). This means that the electron jumping from one lamina to the other occurs with ease.

The curing pressure for the sample in the unidirectional composite configuration is higher than that of any of the crossply samples (Table 2). Consequently, the thickness is the lowest. As a result, the fiber volume fraction is the highest. However, the contact resistivity of the unidirectional sample is the second highest rather than being the lowest, and its activation energy is the lowest rather than the highest. The low activation energy is consistent with the fact that there is no CTE or curing shrinkage mismatch between the two unidirectional laminae and, as a result, no interlaminar stress between the laminae. This low value supports the notion that the interlaminar stress is important in affecting the activation energy. The high contact resistivity for the unidirectional case can be explained in the following way. In the crossply samples, the pressure during curing forces the fibers of the two laminae to press on to one another and hence contact tightly. In the unidirectional sample, the fibers of one of the laminae just sink into the other lamina at the junction, so pressure helps relatively little in the contact between fibers of adjacent laminae. Moreover, in the crossply situation, every fiber at the lamina–lamina interface contacts many fibers of the other lamina, while in the unidirectional situation, every fiber has little chance to contact the fibers of the other lamina. Therefore, the number of contact points between the two laminae is less for the unidirectional sample than the crossply samples.

By measuring the contact electrical resistance of the interlaminar interface of a unidirectional continuous carbon fiber epoxy-matrix composite during shear, the interlaminar shear process can be monitored in real time [21]. The resistance increases throughout the shear process for a low curing pressure, but decreases in the initial stage of shear for a high curing pressure. The resistance increase is due to delamination and

strain in the interface region during shear. The resistance decrease observed for a high curing pressure is believed to be due to interlaminar rubbing and slight damage of the matrix between the fiber layers and the consequent increase in the number of contacts between fibers of the adjacent laminae. The interlaminar displacement is negligible prior to shear failure.

The contact electrical resistivity of the interlaminar interface can be used to monitor thermal damage in a continuous carbon fiber epoxy-matrix composite in real time during thermal cycling [22]. The resistivity increases in spikes and its baseline shifts due to thermal damage.

4. Composite fabrication process

Continuous fiber polymer-matrix composites with thermosetting matrices are important structural materials due to their high strength, high modulus and low density. These composites are commonly made by stacking up layers of fiber prepreg and subsequent consolidation and curing under heat and pressure. Consolidation involves the use of pressure to bring the fiber layers closer to one another and the use of heat to melt the resin in the prepreg, so that the resin flow will allow the layers to come even closer together. A fraction of the resin may be squeezed out during consolidation. Curing occurs subsequent to consolidation and involves the resin completing its polymerization reaction so that it sets. Curing requires sufficient time and temperature in addition to the recommended pressure for curing. There has been much work on the curing process [45–50], but little or no work on the consolidation process. As consolidation is an important step in the composite fabrication process, understanding of the consolidation process and characterization of the effectiveness of consolidation are valuable.

During consolidation, the thickness of the prepreg stack decreases. However, thickness change does not provide information on the extent of interaction between the prepreg layers. In the case of the fibers being carbon fibers, which are electrically conducting, the interaction between the prepreg layers leads to contact between fibers of adjacent layers, thereby causing the volume electrical resistivity in the through-thickness direction (direction perpendicular to the plane of the layers) to decrease. Hence, the resistivity provides information on the extent of fiber–fiber contact. In [19] this resistivity was measured during consolidation for the purpose of studying the consolidation process in detail. Measurement of the resistivity requires measurement of the resistance as well as the thickness.

The through-thickness resistance (R) together with the sample thickness (d) gives the through-thickness resistivity (ρ) according to the equation

$$\rho = R\frac{A}{d}, \tag{2}$$

where A is the area of the sample in the plane of the laminate. This area was assumed to be constant during consolidation and curing.

Let the total through-thickness resistance at a certain time during consolidation be R and that at the start of consolidation be R_0. Let the average resistance of each through-thickness conduction path be R_i. Since the various through-thickness conduction paths are electrically equivalent to resistors in parallel, the total resistance R is given by

$$R = \frac{R_i}{N}. \tag{3}$$

At the start of consolidation, the resistance is

$$R_0 = \frac{R_i}{N_0}. \tag{4}$$

The change in resistance during consolidation is given by

$$\Delta R = R - R_0 = \frac{R_i}{N} - \frac{R_i}{N_0}. \tag{5}$$

Thus

$$\frac{\Delta R}{R_0} = \frac{N_0}{N} - 1 \tag{6}$$

or

$$\frac{N}{N_0} = \frac{R_0}{\Delta R + R_0}. \tag{7}$$

Hence, N/N_0 can be calculated from R_0 and ΔR, which was measured during consolidation, using Eq. (7).

Fig. 8 shows the variation of the through-thickness electrical resistivity and N/N_0 during consolidation at a pressure of 0.56 MPa. During consolidation, the

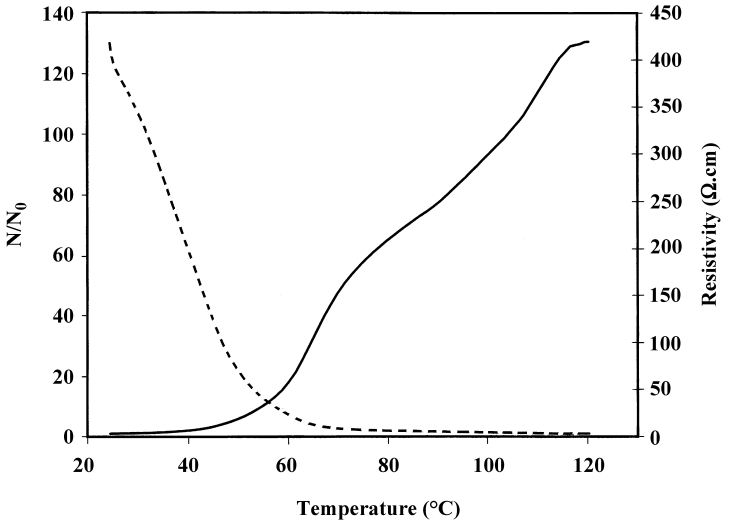

Fig. 8. Variations of N/N_0 (solid line) and through-thickness electrical resistivity (dashed line) with temperature during consolidation heating to 120°C at a pressure of 0.56 MPa.

temperature was raised linearly and reached 120°C, which was the curing temperature. In Fig. 8, the resistivity decreased and N/N_0 increased during consolidation, such that the N/N_0 curve revealed three stages of consolidation. The first stage was characterized by a very gradual increase in N/N_0 (due to the solid form of the resin); the second stage was characterized by an abrupt increase in N/N_0 (due to the molten form of the resin); the third stage was characterized by a moderately gradual increase in N/N_0 (due to the thickening of the resin as the temperature increased). Similar changes in curvature of the N/N_0 plot were observed for consolidation conducted at ramped temperatures that reached 100, 110, 120, 130 or 140°C, although only the results for a maximum temperature of 120°C are shown in Fig. 8. Similar effects were also observed at a pressure of 1.10 MPa. The curve of N/N_0 vs. temperature was quantitatively quite independent of the maximum temperature of consolidation, but was quantitatively different for the two pressures. At the higher pressure, (i) N/N_0 reached much higher values, (ii) the second stage began and ended at higher temperatures, and (iii) the slope of the N/N_0 vs. temperature curve in the second stage was higher ($7.18°C^{-1}$ for 1.10 MPa and $3.31°C^{-1}$ for 0.56 MPa). This means that pressure hastened consolidation and promoted the extent of consolidation, as expressed by the quantity N/N_0. In contrast, increasing the maximum temperature did not promote the extent of consolidation.

5. Residual stress in fiber embedded in matrix

Due to the shrinkage of the matrix during composite fabrication and/or the thermal contraction mismatch between fiber and matrix during cooling near the end of composite fabrication, the fibers in a composite can have a residual compressive stress [51]. This stress may affect the structure of the fiber so that the fiber properties are affected often adversely. It may also cause fiber waviness, which degrades the mechanical properties of the composite.

The measurement of the fiber residual strain by X-ray diffraction, Raman scattering and other optical techniques is difficult due to the anisotropy of the fiber strain and the necessity of embedding the fiber in the matrix. To help alleviate this problem, a method which involves simultaneous electrical and mechanical measurements on the same sample under load has been developed [52]. This method is in contrast to the separate electrical and mechanical measurements.

6. Conclusion

Thermal analysis in the form of the measurement of DC electrical resistance, as conducted on continuous

carbon fiber polymer-matrix structural composites, revealed information on the structural transitions, residual stress, composite interfaces, the composite fabrication process, and thermal damage. The technique was enabled by the electrical conductivity of carbon fibers.

References

[1] J. Mijovic, T.C. Gsell, SAMPE Quart. Soc. Adv. Mater. Proc. Eng. 21 (2) (1990) 42–46.
[2] K.C. Cole, D. Noel, J.-J. Hechler, A. Chouliotis, K.C. Overbury, Polym. Comp. 10 (3) (1989) 150–161.
[3] W.-D. Emmerich, E. Kaisersberger, Materials Science Monographs, Vol. 35, Elsevier, Amsterdam, 1987, pp. 289–297.
[4] W.J. Sichina, P.S. Gill, in: Proceedings of the 41st Annual Conference of Technical Sessions on the Reinforced Plastics, Session. 24, Composites Institute, SPI, New York, 1986, 4 pp.
[5] J.N. Leckenby, D.C. Harget, W.J. Sichina, P.S. Gill, Carbon Fibers: Technology, Uses and Prospects, Noyes Publication, Park Ridge, NJ, 1985, p. 86–99.
[6] J.N. Leckenby, D.C. Harget, W.J. Sichina, P.S. Gill, Carbon Fibers III, Plastics & Rubber Institute, London, UK, 1985, pp. 11.1–11.14.
[7] T.W. Johnson, C.L. Ryan, in: Proceedings of the 31st International SAMPE Symposium and Exhibition 1986: Materials Sciences for the Future, SAMPE, Azusa, CA, 1986, pp. 1537–1548.
[8] D. Wong, J. Jankowsky, M. DiBerardino, R. Cochran, in: Proceedings of the 38th International SAMPE Symposium and Exhibition, Part 2, SAMPE, Covina, CA, 38 (2) (1993) 1552–1565.
[9] K.E. Atkinson, C. Jones, J. Adhesion 56 (1–4) (1996) 247–260.
[10] J.L. Jankowsky, D.G. Wong, M.F. DiBerardino, R.C. Cochran, in: Proceedings of the Symposium on Assignment of the Glass Transition, ASTM, Philadelphia, PA, 1994, pp. 277–292, ASTM Special Technical Publication No. 1249.
[11] P. Olivier, J.P. Cottu, B. Ferret, Composites 26 (7) (1995) 509–515.
[12] A. Licea-Claverie, F.J.U. Carrillo, Polym. Test. 16 (1997) 445–453.
[13] B. Harris, O.G. Graddell, D.P. Almond, C. Lefebvre, J. Verbist, J. Mater. Sci. 28 (12) (1993) 3353–3366.
[14] M. Akay, J.G. Cracknell, H.A. Farnham, Polym. Polym. Comp. 2 (5) (1994) 317–322.
[15] J.W.E. Gearing, M.R. Stone, Polym. Comp. 5 (4) (1984) 312–318.
[16] J.R. Sarasua, J. Pouyet, J. Thermoplastic Comp. Mater. 11 (1) (1998) 2–21.
[17] Z. Mei, D.D.L. Chung, Polym. Comp., in press.
[18] Z. Mei, D.D.L. Chung, Polym. Comp. 19 (6) (1998) 709–713.
[19] S. Wang, D.D.L. Chung, Polym. Comp., in press.
[20] S. Wang, D.D.L. Chung, Comp. Interf. 6 (6) (1999) 497–506.
[21] S. Wang, D.D.L. Chung, Comp. Interf. 6 (6) (1999) 507–518.
[22] S. Wang, D.D.L. Chung, Polym. Compos. in press.
[23] J.A. Kuphal, L.H. Sperling, L.M. Robeson, J. Appl. Polym. Sci. 42 (1991) 1525–1535.
[24] A.L. Simal, A.R. Martin, J. Appl. Polym. Sci. 68 (1998) 453–474.
[25] Ch.R. Davis, J. Appl. Polym. Sci. 62 (1996) 2237–2245.
[26] B.G. Risch, G.L. Wilkes, Polymer 34 (1993) 2330–2343.
[27] H.J. Oswald, E.A. Turi, P.J. Harget, Y.P. Khanna, J. Macromol. Sci. Phys. B 13 (2) (1977) 231–254.
[28] J.U. Otaigbe, W.G. Harland, J. Appl. Polym. Sci. 36 (1988) 165–175.
[29] M.E. Brown, Introduction to Thermal Analysis: Techniques and Application, Chapman & Hall, New York, 1988, p. 25.
[30] C.H. Do, E.M. Pearce, B.J. Bulkin, J. Polym. Sci., Part A 25 (1987) 2409–2424.
[31] M.C. Gupta, S.G. Viswanath, J. Therm. Anal. 47 (4) (1996) 1081–1091.
[32] N. Avramova, Polym. Polym. Comp. 1 (4) (1993) 261–274.
[33] A.L. Simal, A.R. Martin, J. Appl. Polym. Sci. 68 (1998) 441–452.
[34] I.M. Fouda, M.M. El-Tonsy, F.M. Metawe, H.M. Hosny, K.H. Easawi, Polym. Test. 17 (7) (1998) 461–493.
[35] I.M. Fouda, E.A. Seisa, K.A. El-Farahaty, Polym. Test. 15 (1) (1996) 3–12.
[36] L.M. Yarisheva, L. Yu Kabal'nova, A.A. Pedy, A.L. Volynskii, J. Therm. Anal. 38 (5) (1992) 1293–1297.
[37] Y.P. Khanna, Macromolecules 25 (1992) 3298–3300.
[38] Y.P. Khanna, J. Appl. Polym. Sci. 40 (1990) 569–579.
[39] S.D. Incardona, R. Di Maggio, L. Fambri, C. Migliaresi, G. Marom, J. Mater. Sci. 28 (18) (1993) 4983.
[40] ASTM Standard, D 2344-84, 1995, pp. 43–45.
[41] G. Zhou, E.R. Green, C. Morrison, Comp. Sci. Tech. 55 (2) (1995) 187–193.
[42] S.L. Iyer, C. Sivaramakrishnan, C. Young, in: Proceedings of 34th International SAMPE Symposium and Exhibition, Vol. 2, SAMPE, Covina, CA, 1989, pp. 2172–2181.
[43] X. Wang, D.D.L. Chung, Polym. Comp. 18 (6) (1997) 692–700.
[44] A.R. Blythe, Electrical Properties of Polymers, Cambridge University Press, Cambridge, 1980.
[45] C.W. Lee, B. Rice, Int. SAMPE Symp. Exhib. 41 (2) (1996) 1511–1517.
[46] G.M. Maistros, I.K. Partridge, Composite, Part B 29 (3) (1998) 245–250.
[47] R.P. Cocker, D.L. Chadwick, D.J. Dare, R.E. Challis, Int. J. Adh. Adh. 18 (5) (1998) 319–331.
[48] G.R. Powell, P.A. Crosby, D.N. Waters, C.M. France, R.C. Spooncer, G.F. Fernando, Smart Mater. Struct. 7 (4) (1998) 557–568.
[49] Y. Li, S. Menon, Sensors (Peterborough, NH) 15 (2) (1998) 14,16,18–19.
[50] R. Casalini, S. Corezzi, A. Livi, G. Levita, P.A. Rolla, J. Appl. Polym. Sci. 65 (1) (1997) 17–25.
[51] Y. Huang, R.J. Young, Composites 26 (8) (1995) 541–550.
[52] X. Wang, D.D.L. Chung, Comp. Interf. 5 (3) (1998) 277–281.